

Quantum mechanical calculations of amino pyrazole derivatives as corrosion inhibitors for zinc, copper and α -brass in acid chloride solution

A. G. GAD ALLAH, H. MOUSTAFA

Department of Chemistry, Faculty of Science, Cairo University, Giza, Egypt

Received 26 March 1991; revised 17 October 1991

Quantum mechanical calculations have been applied to a series of pyrazole derivatives used as corrosion inhibitors for zinc, copper and α -brass in order to assess quantum chemistry as a means of evaluating effectiveness of corrosion inhibitors. The corresponding structures have been optimized and the energies and coefficients of their molecular orbitals (HOMO and LUMO) have been computed using the semi-empirical method, MNDO. The theoretical results are then compared with experimental data.

1. Introduction

It is known that the efficiency of an organic compound as corrosion inhibitor depends not only on the structure of the inhibitor itself, but also on the characteristics of the environment in which it acts, the nature of the metal surface and the electrochemical potential at the interface [1]. Many organic inhibitors promote the formation of a chelate on the metal surface and, consequently, inhibit the corrosion process [2]. Under such conditions, for a given metal, the efficiency of the inhibitor depends on the stability of the formed chelate. The inhibitor molecule should have centres capable of forming bonds with the metal surface via electron transfer. Thus, the metal acts as an electrophile, whereas the inhibitor molecule acts as a Lewis base, whose nucleophilic centres are normally heteroatoms with free electron pairs which are readily available for sharing, i.e. formation of a bond.

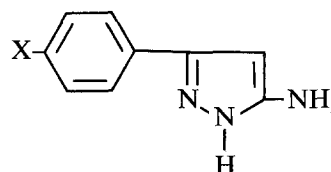
Among the organic compounds used as corrosion inhibitors, amino pyrazole derivatives were found to inhibit the corrosion of zinc [3], α -brass [4] and copper [5] in acid chloride solutions. The inhibition efficiency depends on the substituent type, whether an electron-donating or electron-withdrawing group, and the concentration of the inhibitor [6]. The aim of this paper is to investigate the applicability of quantum mechanical calculations to predict the inhibition efficiency of such a series of amino pyrazole compounds. For this purpose, the structures of such compounds have been optimized and, furthermore, the energies and coefficients of their MO's, net charges on their active centres, gap between HOMO and LUMO, heat of formation, ionization potential and dipole moments have been calculated. The correlations between such parameters and inhibition efficiency for zinc, copper and α -brass in acid chloride solutions have been illustrated.

2. Experimental details

The electrodes of Zn and Cu were cut from spectro-

scopic pure metal rods while that of α -brass was manufactured from local commercial grade brass supplied by the Helwan Company of Non-Ferrous Industries, Egypt with the following composition: Cu, 67.28%; Pb, 0.029%; Fe, 0.002%; Zn, 32.689%.

The preparation of the electrodes, the electrolytic cell, the electric circuit and other experimental details have been given elsewhere [7-9]. All solutions were prepared from AnalaR grade chemicals and triply distilled water. The organic inhibitors used were; 3(5) amino, 5(3)-phenylpyrazole (PP); 3(5) amino, 5(3)[4'-methoxyphenyl] pyrazole (MePP); 3(5) amino [4'-methoxyphenyl] pyrazole (MeOPP); and 3(5) amino, 5(3)[4'-chlorophenylpyrazole] (CIPP). Their structures are as follows:



where X = H(PP), X = CH₃(MePP), X = OCH₃ (MeOPP) and X = Cl(CIPP).

These compounds were prepared, purified and identified following the recommended method [10].

3. Method of calculation

All the quantum mechanical calculations were carried out using the Dewar LCAO-SCF MO semi-empirical method, MNDO (modified neglect of differential overlap). This method develops the MO on a valence basis set.

4. Results and discussion

Figure 1 shows the geometric parameters of the parent amino pyrazole compound, i.e. 3(5) amino, 5(3)-phenylpyrazole (PP), and those for the p-Cl, p-CH₃ and p-OCH₃ derivatives are given in Table 1. As can

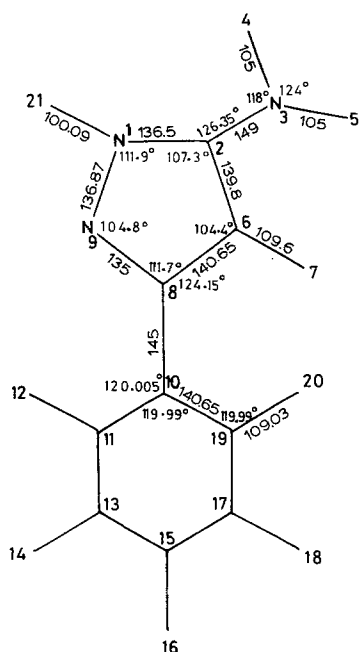


Fig. 1. The geometric parameters of parent amino pyrazole derivative (PP).

be seen from Fig. 1 the active centres of the pyrazole molecule are the two nitrogen atoms of the pyrazole ring (N_1 and N_9) and the nitrogen atom of the amino group (N_3). The coefficients and nodal properties of the two highest occupied molecular orbitals (HOMO and NHOMO) for the pyrazole derivatives are given in Fig. 2. The computed MO coefficients show the contribution of each AO to the probability density of the electronic charge in a given MO. It might be supposed that the HOMO of each molecule could be

Table 1. Geometric parameters for the amino pyrazole derivatives

Amino pyrazole derivative	Bond length /pm	Bond angle /deg.
p-Cl	$b = 174.81$	$\langle ab = 120.067$
p-CH ₃	$b = 151.03$ $c = 110.88$ $d = e = 109.97$	$\langle ab = 120.614$ $\langle bc = 112.39$ (in plane) $\langle bd = 110.833$ out of plane with dihedral angle = 120.07 $\langle be = 110.833$ out of plane with dihedral angle = 239.93
p-OCH ₃	$a = 140.65$ $b = 136.20$ $c = 140.65$ $d = 110.88$ $e = f = 111.0$	$\langle ab = 114.688$ $\langle bc = 124.382$ $\langle cd = 112.39$ (in plane) $\langle ce = 110.833$ out of plane with dihedral angle = 60.636 $\langle cf = 110.833$ out of plane with dihedral angle = 239.93

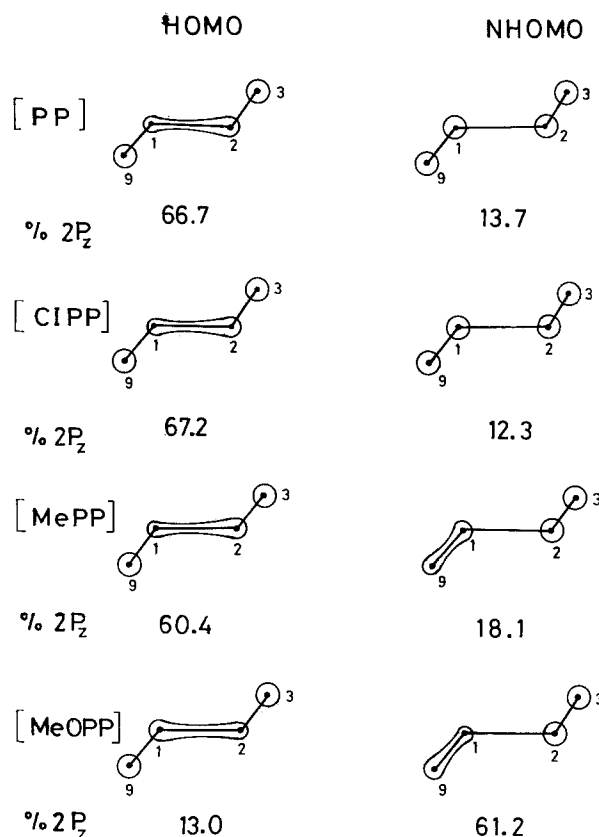
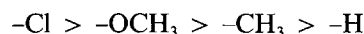


Fig. 2. MO coefficients and nodal properties of the amino pyrazole derivatives.

identified with the free electronic pair of the O or N atom. In the compounds under investigation the identity of the free pair is lost. Thus the HOMO and NHOMO are essentially a linear combination of the 2 p_z orbitals.

On introducing an electron-donating group, e.g. $-\text{CH}_3$ or $-\text{OCH}_3$, into the phenyl group of the pyrazole molecule, the coefficient percent of HOMO decreases while that of the NHOMO increases. Therefore, both MO's may contribute significantly to the charge-transfer. On the other hand, in the case of electron-withdrawing groups, e.g. $-\text{Cl}$, the coefficient percent of HOMO increases while that of NHOMO decreases showing abnormal properties. The coefficient percent for the different amino pyrazole derivatives follows the order:



Such an order is in reasonable agreement with that obtained from polarization measurements, cf. Fig. 3 as an example. The variation of the inhibition efficiency for the different amino pyrazole derivatives with substituent Hammett constants, σ , [12, 13] (for p-chloro, methyl and methoxy, they are +0.23, -0.17 and -0.27, respectively), for the different electrodes are shown in Fig. 4. The correlations are linear and obey an equation similar to that of Hammett, thus:

$$I\% = \rho\sigma \quad (1)$$

where ρ is the proportionality constant which depends

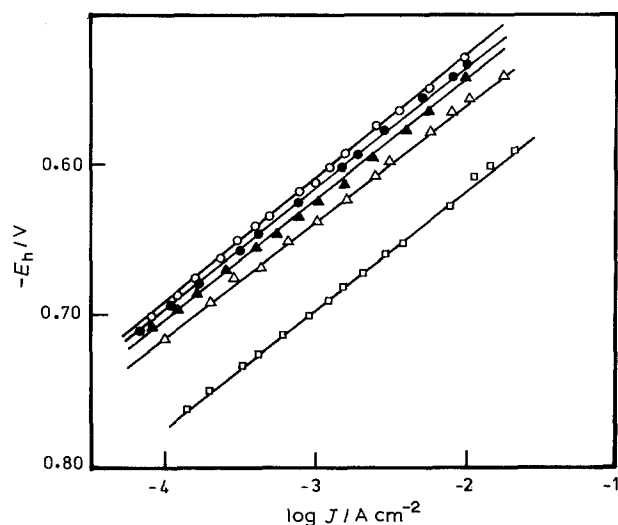


Fig. 3. Anodic polarization of zinc electrode in 0.06 M HCl solutions containing 1×10^{-3} M inhibitor of different substituent: (□) O, (△) PP, (▲) MePP, (○) CIPP and (●) MeOPP. Note: J = current density.

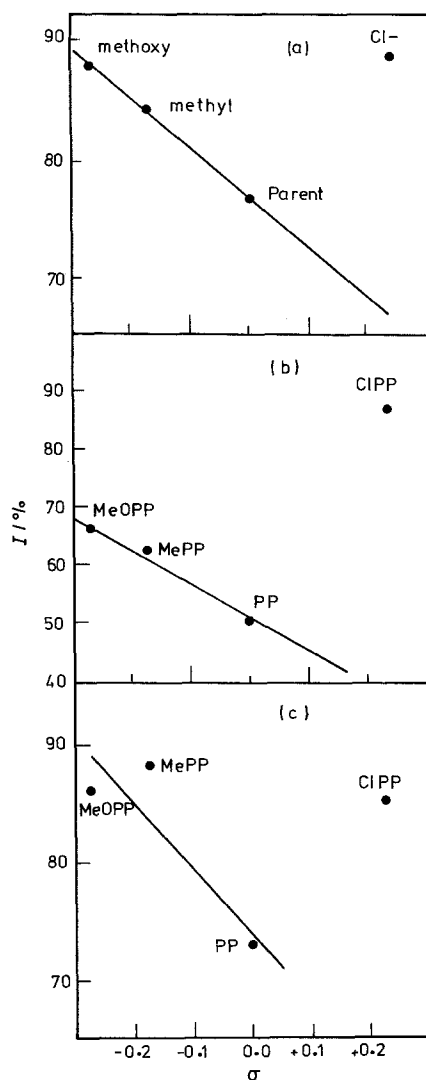


Fig. 4. Variation of inhibition percentage, $I\%$, with Hammett substituent constant, σ , for electrodes of (a) zinc, (b) copper; (c) α -brass.

on the nature of the metal and the electrolyte, respectively; it is a measure of the ability of a given series of inhibitors to reduce corrosion reactions.

Another point regarding MO energy level is the energy gap between the HOMO and LUMO for the different amino pyrazole derivatives. Fischer and Henriksson [14] found that the energy gap, ΔE , is defined as

$$\Delta E = E_{\text{LUMO}} - E_{\text{HOMO}} \quad (2)$$

where E_{LUMO} and E_{HOMO} are the energy of the lowest unoccupied and highest occupied molecular orbitals, respectively. ΔE can be used as a characteristic quantity for metallic complexes. Cherry *et al.* [15] have used the concept of the HOMO-LUMO gap in developing a theoretical model capable of qualitatively explaining the structure stability and conformation barriers in many molecular systems. Furthermore, the energy gap may be related to the redox potential and the electrical resistivities of the complexes [16]. Table 2 shows ΔE values for the different amino pyrazole derivatives. As can be seen ΔE increases on going from the p-chloro derivative to that of the unsubstituted pyrazole molecule (PP). Also, as the MO gap energy increases the efficiency of a compound to inhibit the corrosion process decreases, which reflects the experimental results, *cf.* Fig. 3. Accordingly, the efficiency of the amino pyrazole derivatives as corrosion inhibitors follows the order: $\text{Cl} \approx \text{OCH}_3 > \text{CH}_3 > \text{H}$ which is similar to that observed experimentally.

The charge densities on the active centres for the various amino pyrazole derivatives at their equilibrium geometry, *i.e.* the three nitrogen atoms of the amino group and pyrazole ring, are presented in Table 3. It is seen that the chloro-derivative possesses a new active centre, *i.e.* Cl in addition to the other 3 nitrogen atoms. Also, the calculated charge densities show that the N_3 active centre, the $-\text{NH}_2$ group, is the most probable centre of protonation or chelation. The variations of the net charge densities on each active centre, *i.e.*, N_1 , N_3 and N_9 , respectively, with the Hammett substituent constant, σ , [12, 13] are shown in Fig. 5a-c. The correlations are linear and obey an equation similar to that observed previously, Equation 1, thus:

$$q = \rho' \sigma \quad (3)$$

The proportionality ρ' is small for N_3 and higher for N_1 . It is a measure of the extent to which the active centre contributes in the inhibition process.

A molecular property closely related to the charge distribution in the molecule is the change in the electric dipole moment, μ , caused by the introduction of the substituent group. A recent approximate self-consistent molecular orbital theory (MNDO) is used to calculate the electronic dipole moments of the amino pyrazole derivatives. The nuclear coordinates are chosen to correspond to the standard geometrical model. Within the MNDO, the dipole moments are calculated as the sum of two contributions [17], thus:

$$\mu = \mu_{\text{charged}} + \mu_{\text{hybridized}} \quad (4)$$

Table 2. MO energies and HOMO-LUMO energy gaps for the different amino pyrazole derivatives

Amino pyrazole derivative	E_{HOMO} /eV	E_{LUMO} /eV	$\Delta E = E_{LUMO} - E_{HOMO}$ /eV
PP(H)	-8.7312	0.1170	8.8483
MePP(p-CH ₃)	-8.7397	0.0515	8.7913
MeOPP(p-OCH ₃)	-8.4917	0.1276	8.6193
CIPP(p-Cl)	-8.9029	-0.2797	8.6232

The first contribution, μ_{charged} , is obtained from the net charges located at the nuclear positions. The second contribution, $\mu_{\text{hybridized}}$, is essentially a hybridization term and measures the contribution due to displacement of charge away from the centre of the nuclear position. The dipole moment for the different amino pyrazole derivatives are listed in Table 4. As can be seen the nature of the substituent group affects the dipole moment value of the amino pyrazole compound, the higher value is obtained for the chloro-derivative and the lowest for the unsubstituted one (PP). The order of increase $-\text{Cl} > -\text{OCH}_3 > -\text{CH}_3 > -\text{H}$, is in reasonable agreement with results of the gap energy.

The values of the heat of formation, ΔH_f in kcal mol⁻¹, ionization potential, E_{IP} in eV, and the total energy, E_T in eV, for the different amino pyrazole derivatives support the previous conclusions obtained, *cf.* Table 4. Their correlations with the Hammett substituent constants, σ , are shown in Fig. 6a-d. The relations are linear and obey an equation similar to that of Equations 1 and 3. Therefore, the different parameters obtained from quantum mechanical calculations are in reasonable agreement with the experimental result for the inhibition efficiency of the studied amino pyrazole derivatives as corrosion inhibitors for zinc, copper and α -brass in acid chloride solutions.

5. Mechanism of inhibition

The corrosion of zinc, copper and α -brass in acid chloride solutions is an electrochemical process and its inhibition may take place by changes in corrosion potential or polarization measurements, *i.e.* cathodic or anodic or both. All inhibitors under investigation affect the cathodic and anodic processes [3, 4], to an extent depending on the nature of the metal under test.

The experimental results, *cf.* Figs 3 and 4, show that the inhibition by amino pyrazole derivatives is due to adsorption of the inhibitor molecules on the active anodic and cathodic sites. The nature of the sub-

stituent group affects the inhibition efficiency of the inhibition as is obvious from the net charge on the active centres of the amino pyrazole molecule and other parameters obtained from quantum mechanical calculations, *cf.* Tables 3 and 4. The inhibition action occurs via chelation of the active centres with the metal surface. Further, the chloro-derivative adds a new active centre to the already active centres present in the amino pyrazole molecule which increases its inhibition efficiency. The position of the substituent group with respect to the pyrazole ring also affects the inhibition efficiency of the inhibitor molecules, *i.e.* the para, meta or ortho positions of the arylazo group [6].

Conway and Barradas [18] showed that the inhibition action of pyridine on a mercury surface in 0.5 M HCl solution occurs through adsorption via the lone pair of electrons of the pyridine ring. The same mode of adsorption was also assumed by Smialowska and Kaminski [19], and Fouda *et al.* [20] for thiophene derivatives.

Table 3. Net charge densities on active centres of the amino pyrazole derivatives

Amino pyrazole derivative	N_1	N_3	N_9
H(PP)	-0.1845	-0.4362	-0.1306
p-CH ₃ (MePP)	-0.1822	-0.4365	-0.1316
p-OCH ₃ (MeOPP)	-0.1826	-0.4367	-0.1345
p-Cl*(CIPP)	-0.1802	-0.4353	-0.1280

* The net charge density on Cl- is -0.1092

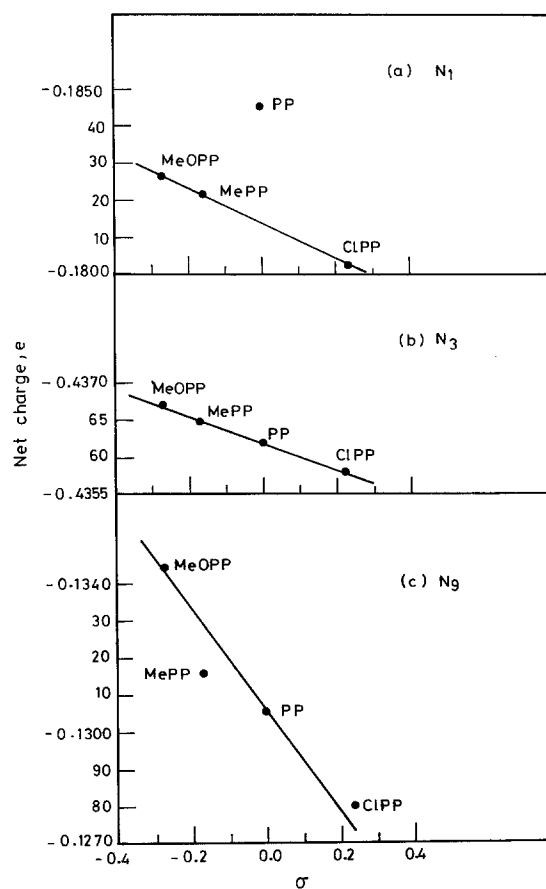


Fig. 5. Variations of the net charge densities on each active centre for amino pyrazole derivatives with Hammett substituent constant.

Table 4. The calculated dipole moment, μ , heat of formation, ΔH_f , ionization energy, E_{IP} and total energy, E_T , for the different amino pyrazole derivatives

Amino pyrazole derivative	Dipole moment, D		Total	Heat of formation /k cal mol ⁻¹	Ionization potential /eV	Total energy /eV
	point charge	hybridized				
H(PP)	1.9120	1.1786	2.9484	97.1411	8.7312	-1896.9203
p-CH ₃ (MePP)	1.9116	1.2268	3.0039	90.1822	8.7398	-2053.4642
p-OCH ₃ (MeOPP)	2.0433	1.6187	3.5606	60.2057	8.4917	-2375.2152
p-Cl(CIPP)	4.0272	1.1346	4.8955	89.6199	8.9029	-2237.4756

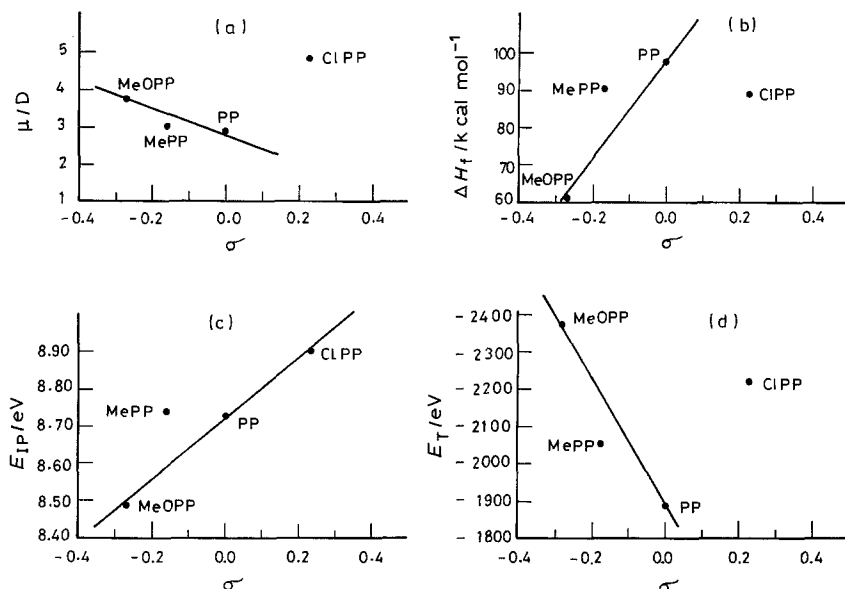


Fig. 6. Hammett plots for the different amino pyrazole derivatives. (a) dipole moment, (b) heat of formation, (c) ionization potential and (d) total energy.

References

- [1] O. L. Riggs, Jr., K. Morrison and D. A. Brunzell, *Corrosion* **35** (1979) 356.
- [2] O. L. Riggs, Jr., 'Corrosion Inhibitors', NACE, Houston, Texas (1973) Chap. 2, pp. 7-27.
- [3] A. G. Gad Allah, M. M. Hefny, S. A. Salih and M. S. El-Basiouny, *Corrosion* **45** (1989) 574.
- [4] A. G. Gad Allah, M. W. Badawy, H. H. Rehan and M. M. Abou-Romia, *J. Appl. Electrochem.* **19** (1989) 928.
- [5] *Idem*, *Indian Journal of Technology* (1990), accepted for publication.
- [6] A. G. Gad Allah and H. M. Tamous, *J. Appl. Electrochem.* **20** (1990) 488.
- [7] A. G. Gad Allah, W. A. Badawy and H. H. Rehan, *Ibid* **19** (1989) 768.
- [8] A. G. Gad Allah and A. A. Mazhar, *Corrosion* **45** (1989) 381.
- [9] A. G. Gad Allah and H. A. Abd El-Rahman, *Indian Bull. Electrochem.* **6** (1990) 658.
- [10] A. Takamizawa and Y. Hamashima, *Yakugaku Zasshi (Jpn)* **48** (1964) 1113.
- [11] M. J. S. Dewar and W. Thiel, *J. Am. Chem. Soc.* **99** (15) (1977) 4899.
- [12] O. Reutov, 'Theoretical Principles of Organic Chemistry' Mir Publishers, Moscow (1967).
- [13] R. A. Y. Jones, 'Physical and Mechanistic Organic Chemistry', Cambridge University Press, Cambridge, UK (1979).
- [14] I. Fischer-Hjalmars and A. Henriksson-Enflo, *Adv. Quantum Chem.* **16** (1982) 1.
- [15] W. Cherry, N. Fpitiis and W. Thatcher Borton, *Acc. Chem. Res.* **16** (1977) 167.
- [16] E. J. Rosa and G. Schrauzer, *J. Phys. Chem.* **73** (1969) 2432.
- [17] J. A. Pople and G. A. Segal, *ibid.* **43** (1965) S136.
- [18] B. E. Conway and R. G. Barradas, *Electrochim. Acta.* **5** (1961) 319.
- [19] Z. S. Smialowska and M. Kaminski, *Corros. Sci.* **13** (1973) 1.
- [20] A. S. Fouda, H. M. Abu-Elnader and M. S. Soliman, *Bull. Korean Chem. Soc.* **7** (1986) 97.